IEEE Access
Multidisciplinary | Rapid Review | Open Access Journal

Received April 18, 2019, accepted June 22, 2019, date of publication July 10, 2019, date of current version August 13, 2019.

Digital Object Identifier 10.1109/ACCESS.2019.2927882

Annealing Effects on XLPE Insulation of Retired High-Voltage Cable

YUE XIE[1], (Student Member, IEEE), YIFENG ZHAO[1], GANG LIU[1], JIASHENG HUANG[2], AND LICHENG LI[1]

[1]School of Electric Power, South China University of Technology, Guangzhou 510640, China
[2]Transmission Management Office, Guangzhou Power Supply Bureau, Guangzhou 510640, China

Corresponding author: Gang Liu (liugang@scut.edu.cn)

ABSTRACT In this paper, the performance of several annealing methods on three retired cables and the annealing effects on the improvement in the thermal and electrical properties of cross-linked polyethylene (XLPE) insulation were discussed. The cable insulation layer was peeled, and the peels near the inner semi-conductive layer were used as the test samples. Isothermal treatment and heat recycling treatment were performed at temperatures of 85, 90, 95, and 100 °C, and the temperatures were held in the heat recycling treatment for 8, 16, and 24 h, respectively. Each heat recycling treatment was repeated 20 times, and the duration of the isothermal treatment was the same as that for the heat recycling treatment with a 24 h temperature holding hour. Then, Fourier transform infrared spectroscopy (FTIR) and differential scanning calorimetry (DSC) were performed, and the dielectric spectrum, DC conduction current, and dielectric breakdown strength E_B were measured. The results showed that damage involving molecular changes is linearly related to the cable service year. As the annealing temperature increases, the melting range and electrical conductivity decrease; the melting point, crystallinity, lamellar thickness, and dielectric breakdown strength increase; and the optimal values appear for the samples annealed at 95 °C. With an increased temperature holding hour, the peels annealed at 95 °C exhibit a decreased melting range and electrical conductivity and an increased crystallinity, melting point, lamellar thickness, and dielectric breakdown strength. As a result, the two different treatments are verified to effectively improve the thermal and electrical properties for the XLPE as early research on cable rejuvenation by heat treatment.

INDEX TERMS XLPE, DSC, DC current, dielectric breakdown strength, dielectric spectrum.

I. INTRODUCTION

Cross-linked polyethylene (XLPE) has been widely used as the insulation material in high-voltage cables due to its excellent electrical properties and environmentally-friendly nature. During long-term operation, insulation degradation inevitably occurs from multiple pressures, including thermal, electrical, and mechanical effects, which threatens cable operation safety. Much research has been conducted on cable insulation degradation, and the aging mechanism and its evolution process under different settings have been well investigated [1], [2]. Some research has focused on providing an accurate assessment of cable aging and determining whether a cable should continue to operate or be retired and replaced by a new cable [3], [4]. Although many methods and measurement techniques have been shown to be effective in the aging assessment of XLPE peels and coaxial cables, complex cable-laying conditions and various sources of interference in the on-site environment can render such measurement results invalid [5], [6].

Annealing is a heat treatment method that is widely used in the research on crystalline polymer materials. Two annealing methods, isothermal treatment and thermal cycling treatment, have shown the ability to improve the thermal and electrical properties of XLPE at proper temperatures [7], [8]. Over the short timescale of the cable manufacturing period, the crystal-amorphous structure does not reach the metastable state. Thus, annealing occurs at a temperature above the glass transition temperature during cable operation, and the evolution of the crystal-amorphous structure in the insulation layer has been widely observed in retired cables [9], [10]. For example, cables that have operated for nearly 15 years show enhanced

The associate editor coordinating the review of this manuscript and approving it for publication was Boxue Du.

TABLE 1. Important specifications of the selected three cables.

Sample	M_I	M_C	d_{IS}	d_I	d_{OC}	S_C	O_P
XLPE-0	XLPE	Cu	2	19.8	2	700	-
XLPE-15	XLPE	Cu	2	19.8	2	700	2000-2015
XLPE-30	XLPE	Cu	2	19.8	2	700	1985-2015

M_I: insulation material, M_C: conductor material, d_{IS}: inner semiconductor thickness in mm, d_I:insulation thickness in mm, d_{OC}: outer semiconductor thickness in mm, S_C: conductor area in mm^2, O_P: operation period. Other parameters such as cross-linking method are unknown.

thermal and electrical properties compared to new cables. The reason for the enhancement has been summarized as a ''second annealing process'', with molecular chains forming an orderly arrangement, imperfect crystals being converted to perfect ones, thin lamellae becoming thick lamellae, and new crystal formation accompanying a reduction in the amorphous region [11]. When cables reach the designed service life, the insulation degradation would dominate this process [10]. Although some research has evidenced cables that have maintained excellent electrical properties, their further operation would have a high probability of serious insulation failure, and an effective method of evaluating the insulation property of these cables is not currently available [12], [13].

In this study, two different annealing methods are performed on XLPE sheets peeled from three retired cables with 0, 15, and 30 years of service. The effects of annealing on the thermal and electrical performance of the XLPE sheets are analyzed. The effectiveness of the different annealing methods was compared, and the possibility for cable rejuvenation was discussed in a preliminary manner.

II. EXPERIMENTAL DETAILS

A. SAMPLE PREPARATION

Three 110 kV AC cables were used in the present study, and some important specific parameters are listed in Table 1. Two of the cables were retired cables that operated for 15 and 30 years, and the last cable was a spare cable. The two retired cables were removed from service because of transmission line change rather than insulation failure. Overheated operation was not reported for the two retired cables, which means that the temperature in the insulation layer remained below 90 °C during cable operation. No physical damage or deformation was observed in the main body of the three cables, and only a few deformation points were found in the outer aluminum sheath.

After removing the outer aluminum sheath, the cable insulation was peeled parallel to the copper conductor surface, and tape-like XLPE peels were obtained, as shown in Figure 1. Peels near the inner semi-conductive layer were taken as the test samples and cut into a square shape with a width of 6 cm, since these locations suffered the most serious electrical and thermal pressures during cable operation. Before the annealing process was conducted,

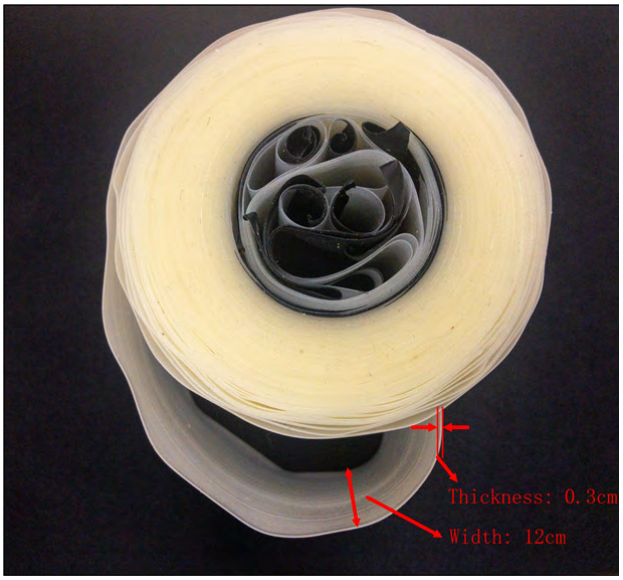

FIGURE 1. Illustration of tape-like XLPE peels.

all samples were wiped clean by ethyl alcohol, and then they were inserted into two thick steel plates and put in a drying oven with the temperature held at 60 °C for 48 h. Each sample was dried and pressed into a plate sheet to ensure good contact in the subsequent measurements.

B. SAMPLE TREATMENT

As is well known, the temperature change in cable insulation is a typical slow and non-isothermal process, including heating and cooling phases [14]. To obtain a good simulation of the heating process, an annealing oven was developed, as shown in Figure 2. In Figure 2(a), the annealing oven is made of iron sheets, and the six surfaces are covered by heat insulation foam of the same thickness. The samples located on the sampling stage and the annealing oven were locked within the heat oven.

First, the chamber of the heat oven is heated to the preset temperature and maintained at that point. Simultaneously, heat is transferred from the chamber of the heat oven to the chamber of the annealing oven through the heat insulation foam, which increases the temperature in the chamber of the annealing oven. After the temperature in the chamber of the annealing oven reaches the preset point and is maintained at that temperature for the temperature holding hour T_h, the heat oven is turned off, and the temperature in the chamber of the heat oven decreases rapidly to room temperature. The temperature in the chamber of the annealing oven decreases with the heat dissipation from the chamber of the annealing oven to the chamber of the heat oven. Two fans that operate continuously are installed at the top and bottom of the chamber of the heat oven to force air circulation. A complete cycle includes a heating, holding, and cooling phase. Figure 2(b) shows the temperature evolution process of a complete cycle at the annealing temperature of 100 °C. The heating rate decreases as the temperature increases in the chamber of the

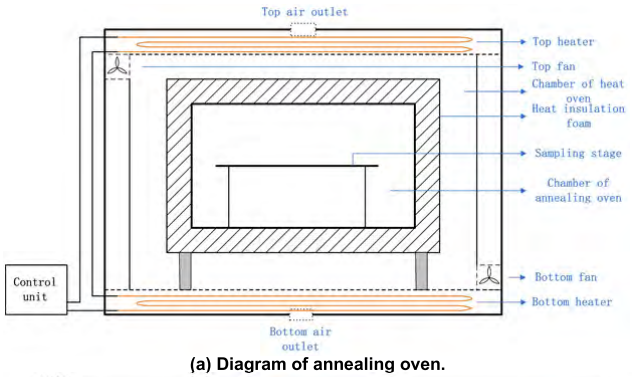

(a) Diagram of annealing oven.

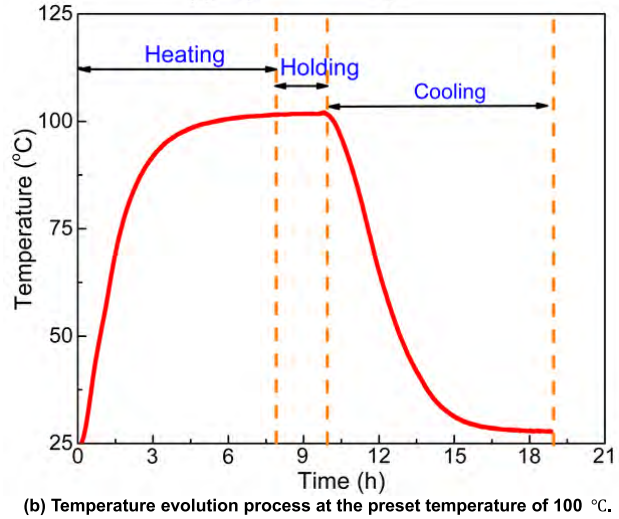

(b) Temperature evolution process at the preset temperature of 100 °C.

FIGURE 2. Experimental settings of heat treatment.

annealing oven, and the cooling rate decreases as the temperature decreases in the chamber of the annealing oven. As far as the coaxial cable is concerned, heat is transferred from the metal conductor to the outside through heat exchange. The temperature in the insulation layer increases by a high current applied in the conductor, and the temperature decreases in the insulation layer when the current in the central conductor is below a certain amplitude. Specifically, the cooling phase depends on the cable's physical structure and the on-site environment, and it could be considered a fixed condition when the cable has been laid well [14].

Two different heat treatment methods are adopted. The first three heat treatments are thermal recycling treatments, with temperature holding hour T_h of 8, 16, and 24 h. The last heat treatment is an isothermal treatment in which the temperature is increased to the preset temperature and maintained until the heat treatment is finished, and the time duration is same as the heat recycling treatment with the T_h of 24 h. Table 2 presents the hours of heating and cooling during the annealing process at different preset temperatures. The same thermal cycle annealing process was repeated for each sample 20 times.

Samples annealed at the same preset temperature with T_h values of 8 h, 16 h, 24 h, and the isothermal treatment are labeled S-1, S-2, S-3, and S-4, respectively, and samples annealed by the same method are named according to their service year: XLPE-0, XLPE-15, and XLPE-30.

TABLE 2. Hours of heating and cooling for annealing.

Preset temperature (°C)	Heating hours	Cooling hours
85	4.2	6
90	6	6.5
95	7.5	8.2
100	8	9

C. PARAMETER MEASUREMENT

The molecular changes in XLPE were analyzed with a Fourier transform infrared spectroscopy (FTIR) spectrometer (VERTEX 70, Bruker, German). Spectra were obtained over the wavelength range 400 $\sim$ 4000 cm^{-1} with a resolution of 4 cm^{-1}. For each sample, the same measurement was repeated 5 times to increase the accuracy of the results, and the displayed FTIR spectra were the averages of 5 FTIR measurements.

Differential scanning calorimetry (DSC) was performed with a Q200 (TA Instruments, USA) instrument to measure the thermal properties of the samples. A sample with a weight of 5 mg was used in each measurement. The temperature was increased from 25 to 140 °C at a rate of 10 °C/min, maintained at 140 °C for 5 min, and then cooled to 25 °C. This scanning was repeated twice per measurement, and 5 measurements were performed for each sample.

The complex permittivity, including the real part (ε') and the imaginary part (ε''), was measured with a QE 200 (Novo-control, Germany) instrument. The frequency range was from 10^{-2} to 10^{6}Hz at the temperature of 90 °C.

The DC conduction current was measured with a three-electrode conduction instrument. An electric field of 20 kV/mm was applied and the current was measured for 1800 s at the same temperature as in the dielectric spectrum measurement.

The dielectric breakdown strength E_B was measured at room temperature by applying an AC (50 Hz) high voltage to a copper plate electrode system. The sample was inserted between two plate electrodes, and completely immersed in silicone oil. The voltage linearly increased at a rate of 1 kV until sample breakdown. The same measurement was repeated 15 times for each sample, and the average was calculated as the final data.

III. RESULTS AND DISCUSSION

A. MOLECULAR CHAIN DAMAGE

Figure 3 shows the FTIR spectra of the three samples without annealing. The peak at the wavelength of 720 cm^{-1} corresponds to rocking methylene groups (-CH_2), and other three peaks, which appear at 1467 cm^{-1}, 2847 cm^{-1}, and 2924 cm^{-1}, are the most characteristics of XLPE, corresponding to the wag vibration, symmetric stretching vibration, and asymmetric stretching vibration of the CH_2 groups, respectively [15]. The peak observed at 1374 cm^{-1} with a low absorbance strength corresponds to the ethyl group, and there

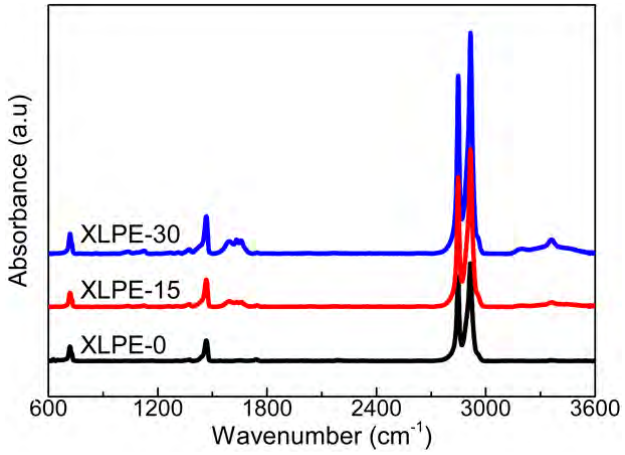

FIGURE 3. FTIR spectra observed for the samples without annealing.

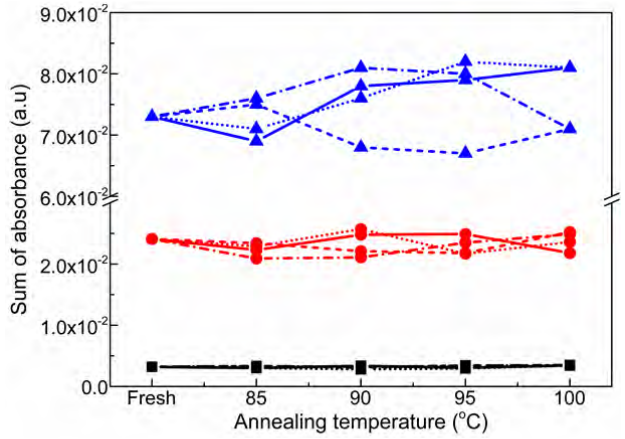

FIGURE 4. Annealing temperature dependence of the sum for the two peaks. Solid symbols (■, ●, ▲) represent XLPE-0, XLPE-15, XLPE-30.

is almost no difference in the three samples [16]. The peak at the wavelength of 1740 cm^{-1} that shows weak absorbance corresponds to the carbonyl group, with almost no increase with the cable service year. This means that oxidation took place during the cable manufacturing process, but long-term operation did not result in any further reaction [17]. As the wavenumber increases, two peaks are observed at 1632 cm^{-1} and 3359 cm^{-1}, corresponding to the unsaturated group and the hydroxyl group [18]. The two peaks appear for only XLPE-15 and XLPE-30, and the absorbance strength is linear with their service year, which strongly evidences that the two samples suffered serious degradation, particularly XLPE-30.

The peaks at 1632 and 3359 cm^{-1}, selected to evaluate the molecular change. The sum of the absorbance of the two peaks was calculated and shown in Figure 4. The changes in the annealing temperature dependence of sum are not clear; only the irregular deviations are observed. The reason seems to be the non-uniform distribution of the molecular chain.

B. THERMAL PROPERTIES

Due to the vast amount of data in the measured DSC spectra for all samples, only the DSC spectra of XLPE-0 are adopted and shown in the following figures.

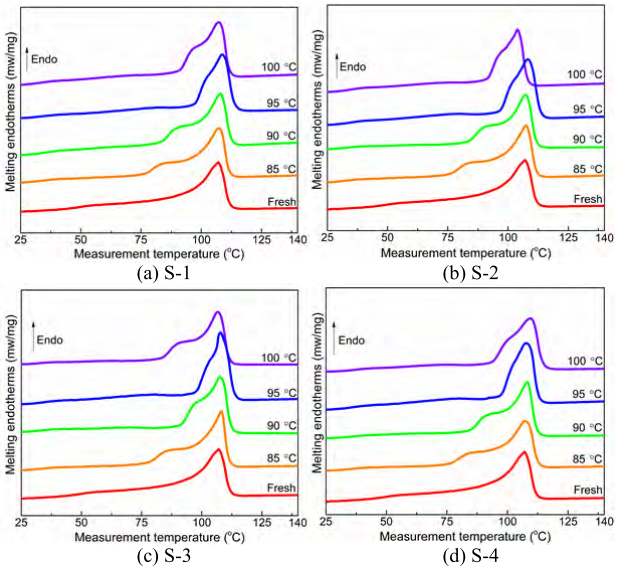

FIGURE 5. Melting endotherms observed for XLPE-0 in the first heating phase.

Figure 5 shows the melting endotherms of XLPE-0 measured in the first heating phase. In each graph, the melting point shifts to a higher temperature and the melting range narrows as the annealing temperature increases. The highest melting point and the smallest melting range are observed when each sample is annealed at 95 °C. Furthermore, the melting point shifts to a lower temperature and the melting range becomes larger when each sample is annealed at 100 °C. The change in the melting range, which is primarily concentrated below the melting point, occurs because many thin lamellae are converted into thicker lamellae, leading to a denser crystal distribution [19]. The melting point corresponding to the thickest lamellae shifts to a higher temperature, which also indicates that the thickest lamellae were thickened further. When each sample is annealed at a higher temperature of 100 °C, the melting point decreases and the melting range broadens as a result of the melting of the thicker lamellae and the emergence of the thinner lamellae [20].

The melting point and melting range in Figure 5 consistently show that the optimal values appear when each sample is annealed at 95 °C, regardless of the temperature holding hour. To clearly illustrate the differences observed for the samples annealed at 95 °C with different T_h, Figure 6 shows the melting endotherms of XLPE-0 annealed at 95 °C by different heat treatment methods. The higher melting point and narrower melting range obviously correspond to a longer T_h. The highest melting point and smallest melting range appear for S-3 and S-4, and it is hard to distinguish between them.

Generally, the melting endotherms in the second heating phase are also highly important. Figure 7 shows the melting endotherms of XLPE-0 measured in the second heating phase. In each graph, each curve shows a similar heat flow at each temperature and the same melting point.

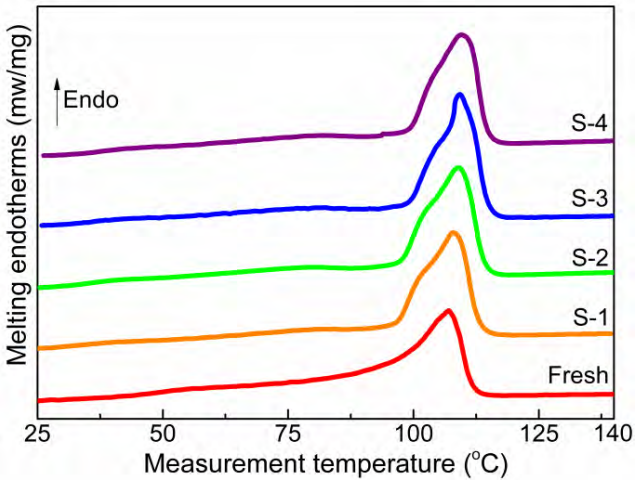

FIGURE 6. Melting endotherms observed for XLPE-0 in the first heating phase with samples annealed at 95 °C.

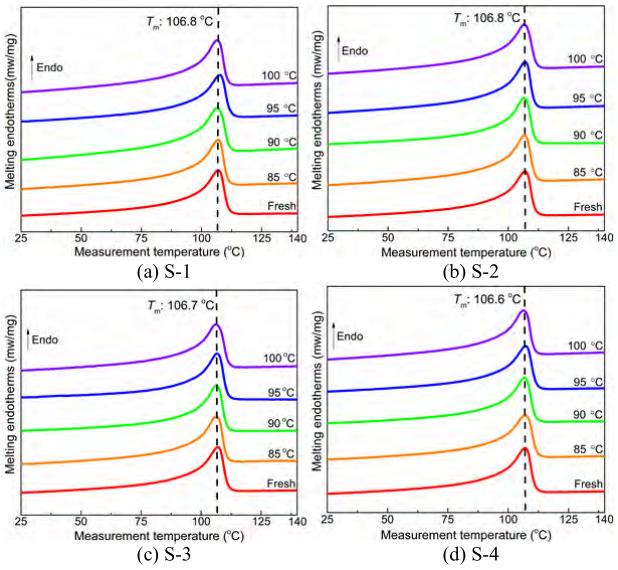

FIGURE 7. Melting endotherms observed for XLPE-0 in the second heating phase.

Slight differences are observed among the four graphs, indicating that similar crystal-amorphous structures form when all crystals are completely melted when the sample is heated to 140 °C in the first heating phase and recrystallized in the first cooling phase. As the sample cools to 25 °C at the same rate, a similar crystal-amorphous structure emerges, which means that there is no change in the molecular chain, indicating that the annealing at these temperatures for hundreds of hours did not further damage the molecular chain [21]. This is consistent with the results shown in Figure 4.

Comparing Figures 5 and 7, the melting endotherms measured in the first heating phase provide more detailed information about the effect of annealing on the thermal properties for the samples. Based on the melting endotherms measured in the first heating phase for all samples, the melting point was obtained directly, and the crystallinity X,

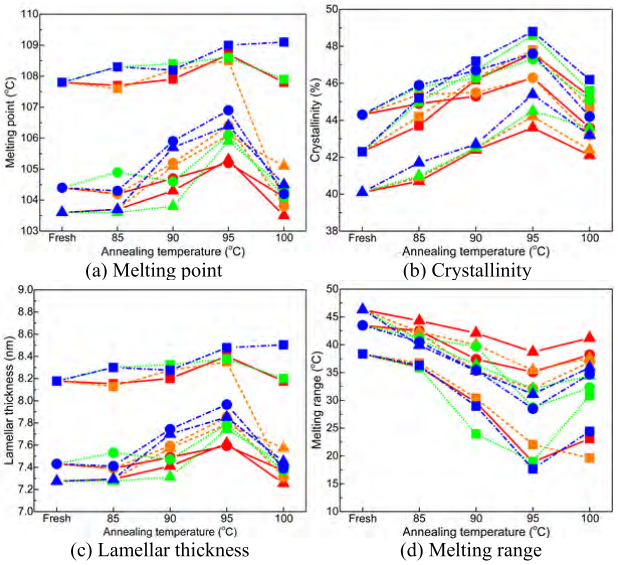

FIGURE 8. Melting point, crystallinity, lamellar thickness, and melting range as a function of annealing temperature. Solid symbols (■, ●, ▲) represent XLPE-0, XLPE-15, XLPE-30. Solid line (——): S-1, short dash line (– –): S-2, short dot line (.....): S-3, short dash dot line (– · –): S-4.

lamellar thickness L, and melting range T_{mr} were calculated using the following three equations [22]–[24],

$$X = \frac{\Delta H_{\mathrm{o}}}{\Delta H_{\mathrm{m}}} \times 100\% \tag{1}$$

$$L = \frac{2\sigma_e T_{\mathrm{m0}}}{\Delta H_{\mathrm{m}}(T_{\mathrm{m0}} - T_{\mathrm{m}})}, \tag{2}$$

$$\text{and } T_{mr} = T_{me} - T_{ms} \tag{3}$$

where ΔH_{o} is the observed fusion enthalpy per unit volume and ΔH_{m} is the value for an ideal polyethylene crystal, 2.88×10^8 J · m^{-3}. Furthermore, T_{m0} is the melting point of polyethylene for an infinitely thick crystal, 414.6 K. In addition, σ_{e} is the surface-free energy per unit area of the basal face, 9.3×10^{-2} J · m^{-2}, T_{ms} is the starting melting point, and T_{me} is the ending melting point.

Figure 8 shows the values of the melting point, crystallinity, lamellar thickness, and melting range as a function of annealing temperature. From Figure 8(a) to (c), the changes in these three values exhibit the same trend: the values increase with the increasing annealing temperature, and the maxima appear at the annealing temperature of 95 °C. The melting range shown in Figure 8(d) decreases with the increasing annealing temperature, and the smallest value appears at the same annealing temperature as the previous three values. For the samples annealed at 100 °C, the former three values decreased identically, and the melting range increased.

The changes in the four factors are sensitive to the annealing temperature, and the optimum temperature here is 95 °C. The relationship between the annealing temperature and the changes in the four values can be interpreted by the master curve derived by Gandica and Magill [25]. When the annealing temperature is below the optimum annealing

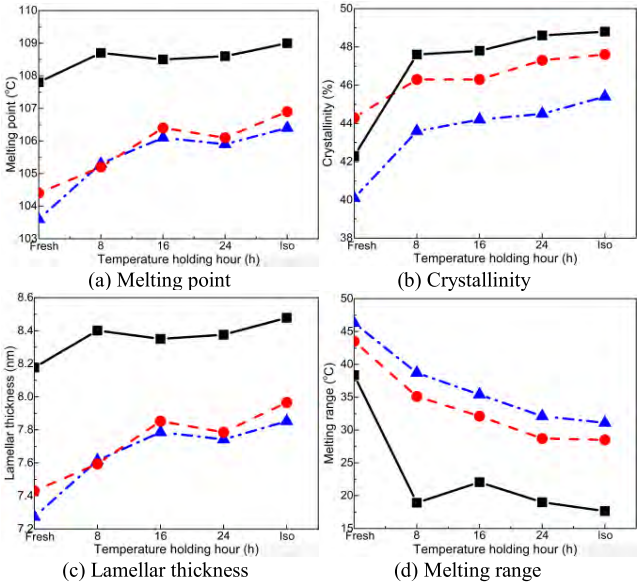

FIGURE 9. The values of melting point, crystallinity, lamellar thickness, and melting range as a function of T_h for the samples annealed at 95 °C. Solid symbols (■, ●, ▲) represent XLPE-0, XLPE-15, XLPE-30. Iso is the abbreviation of isothermal treatment.

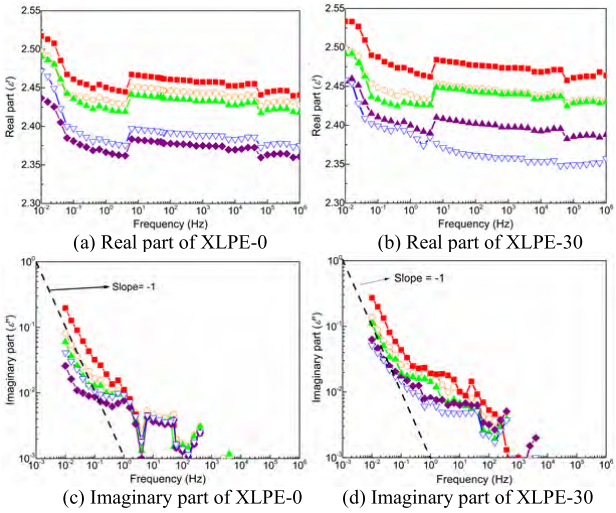

FIGURE 10. Real part ε' and imaginary part ε'' as a function of frequency measured at 90 °C for isothermally annealed samples of XLPE-0 and XLPE-30. Annealing temperature: (■) Fresh, (●) 85 °C, (▲) 90 °C, (▽) 95 °C, (◆): 100 °C.

point, the temperature increase will result in a higher thermal energy and increase the rate of molecular chain arrangement, allowing for long molecular chain movement [26]. This increase favors the thickening of the lamellae and the emergence of new crystals, which dominate this process rather than the crystal melt. When the temperature is above the optimum annealing point, the higher thermal energy accelerates the molecular chain movement, especially for the long chains. However, the free chains hardly arrange into an ordered state, and the ordered chains start to diffuse from the original lamellae [27]. As a result, the original thicker lamellae melt, and new thin lamellae emerge.

To compare the effects of the different heat treatment methods on the thermal properties, Figure 8 shows the values of the melting point, crystallinity, lamellar thickness, and melting range of the samples annealed at 95 °C. The values in Figure 9(a) to (c) increase with the increasing T_h, and the value in Figure 9(d) decreases with the increasing T_h; if we ignore a slight exception, the optimum values are observed in S-4. It is well known that XLPE is an original symmetric molecular chain, polar groups and impurities emerge from degradation, and their movement impedes the crystal emergence [21]–[25]. For the sample annealed at the optimum point, a longer T_h means the longer time for molecular chain movement over larger distances, and gradually, thicker and more uniform lamellae emerge. Compared with the heat recycling treatment, isothermal treatment gives the best results with respect to the thermal properties.

C. ELECTRICAL PROPERTIES

Figure 10 shows the real part ε' and the imaginary part ε'' as a function of frequency measured for the isothermally annealed samples of XLPE-0 and XLPE-30. In each graph, almost no changes in ε' and no regularity in ε'' are observed at frequencies above approximately 1 Hz. At frequencies below approximately 1 Hz, ε' increases dramatically with the decreasing frequency due to the accumulation of hetero charge. When hetero charges accumulate near the electrode, and charges with opposite polarity are induced on the electrode, which increases the real part ε', the resultant phenomenon is called electrode polarization [28], [29]. The imaginary part ε'' at frequencies below approximately 1 Hz increases dramatically with the decreasing frequency due to ion transport to the electrode in the phase of the applied voltage, which generates Joule heat and results in an increase in the imaginary part. In this case, the real part ε' and the imaginary part ε'' below 1 Hz are selected to evaluate the dielectric properties of the samples.

As shown in the upper two graphs of Figure 10, the real part ε' in the measured frequency decreases as the annealing temperature increases, reaching the smallest value for XLPE-30 annealed at 95 °C and XLPE-0 annealed at 100 °C; however, the real part ε' increases for XLPE-30 annealed at 100 °C. In the bottom two graphs of Figure 10, regular changes in the imaginary part are observed when the frequency is below 1 Hz. The changes in the imaginary part in the two graphs show almost the same trend as the changes in the real part: ε'' decreases with the increase in the annealing temperature and reaches the smallest value at the annealing temperature of 95 °C and 100 °C for XLPE-30 and XLPE-0, respectively.

Regarding the ion transport contributions to the increases in the real part and imaginary part at low frequencies, especially below 1 Hz, the contribution of the DC conductivity could be used to analyze the effect of annealing on the behavior of ions. The complex permittivity, including the effects of

the DC conductivity, is given by [29]:

$$\varepsilon^* = \varepsilon_\infty + \frac{\varepsilon_s - \varepsilon_\infty}{1 + j\omega\tau} - j\frac{\sigma_{DC}}{\omega\varepsilon_0} \tag{4}$$

where ε^* is the complex permittivity, ε_s is $\varepsilon'(\omega = 0)$, ε_θ is $\varepsilon'(\omega = \infty)$, ω is the angular frequency ($\omega = 2\pi f$, f is the frequency of the applied electric field), τ is the relaxation time, and ε_0 is the permittivity of vacuum. The third term represents the dielectric loss caused by the DC conductivity, and the DC conductivity is given by [29], [30]:

$$\sigma_{DC} = 2\pi\varepsilon_0 f\varepsilon'' \tag{5}$$

If we change this equation into $Log(\varepsilon'')$ as a function of $Log(f)$, then

$$Log(\varepsilon'') = -Log(f) + Log(\frac{\sigma_{DC}}{2\pi\varepsilon_0}) \tag{6}$$

The slope of the line $Log(\varepsilon'')$ vs. $Log(f)$ fits -1 from this equation, and it is clearly seen that it is a linear function with a slope of -1 at the frequencies between 0.01 and 0.1 Hz, as shown in the bottom two graphs of Figure 10.

Figure 11 shows the results of the DC conductivity σ_{DC} deduced from the complex permittivity. At such a low applied electric field, the ions mainly originate from impurity ionization. In Figure 11(a), σ_{DC} in the three samples decreases as the annealing temperature increases, and the smallest values appear when the samples are annealed at 95 °C. In Figure 11(b), a longer temperature holding hour contributes to a smaller σ_{DC}, and the smallest σ_{DC} appears in S-4, except for a small increase as XLPE-0 is isothermally treated.

Based on the results of the DC conduction current, the DC conductivity σ could be calculated with equations (7) [31], [32],

$$\sigma_{DC} = \frac{I_{av}}{SE} \tag{7}$$

where I_{av} is the average DC current in the last 30 s, S is the electrode area, and E is the strength of the applied electric field.

Figure 12 shows the results of the DC conductivity σ_{DC} from the DC current measurement. At high applied electric fields with 20 kV/mm, which is above the charge injection threshold for XLPE, the charge carriers from the electrode injection would dominate the concentration of the carriers [33]. In the two graphs of Figure 12, a similar phenomenon to that shown in Figure 11 is observed; σ_{DC} for each sample decreases as the annealing temperature increases, reaches the smallest values when the sample is annealed at 95 °C, and the smallest σ appears when the sample is isothermally annealed at 95 °C. Apparently, σ_{DC} from DC current is larger than that deduced from the complex permittivity, due to charge injection.

As is well known, the higher the crystallinity and the thicker the lamellae, the harder the charge carrier transport is in the bulk of the sample [33]. Therefore, the changes in the

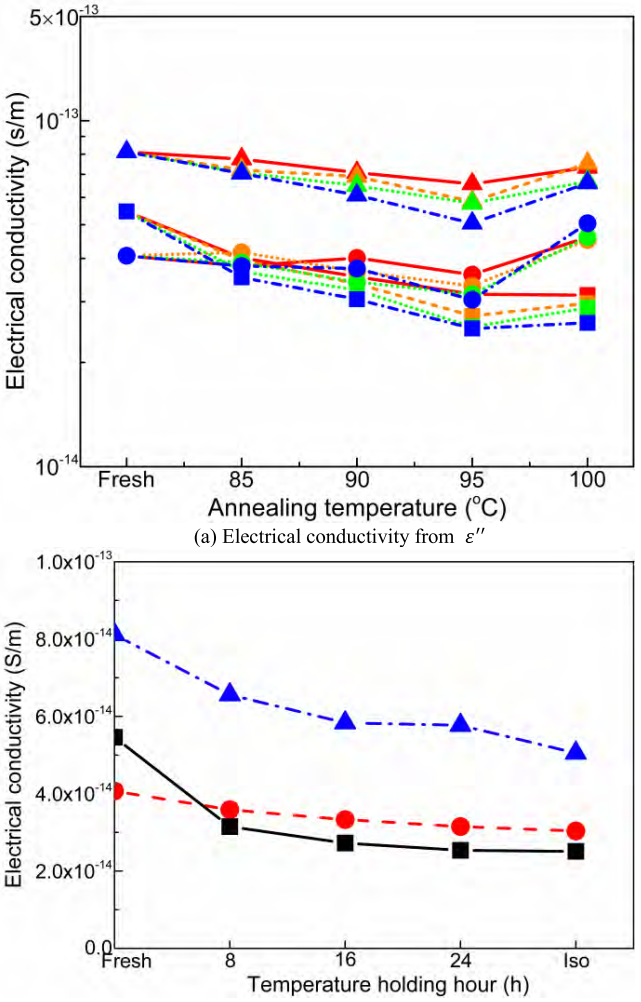

(a) Electrical conductivity from ε''

(b) Electrical conductivity for the samples annealed at 95 °C

FIGURE 11. Electrical conductivity σ_{DC} as a function of annealing temperature. Solid symbols (■, ●, ▲) represent XLPE-0, XLPE-15, and XLPE-30. Solid line (——): S-1, short dash line (– –): S-2, short dot line (.....): S-3, short dash dot line (– . –): S-4. Iso is the abbreviation of isothermal treatment.

two different σ_{DC} values illustrated in Figure 11 and 12 show the same trend as the DSC results.

The dielectric breakdown strength E_B is the most common and valuable parameter in the assessment of the electrical performance for XLPEs. Figure 13 shows the results of E_B observed for all samples. In Figure 13(a), E_B in each sample increases as the annealing temperature increases and reaches the maximum value when the sample is annealed at 95 °C. Figure 13(b) compares the values of E_B for the samples annealed at 95 °C by different heat treatment methods. There is an obvious increase in E_B as T_h increases, and the highest E_B appears in S-4. The charge transfer is harder in the crystalline region, as explained in the results of the DC current measurement. More importantly, the amorphous region facilitates charge transport and generally decreases the dielectric breakdown strength [34]. The increase in crystallinity means that the enlargement of the crystal region and narrowness of the amorphous region, and the annealing process contributes

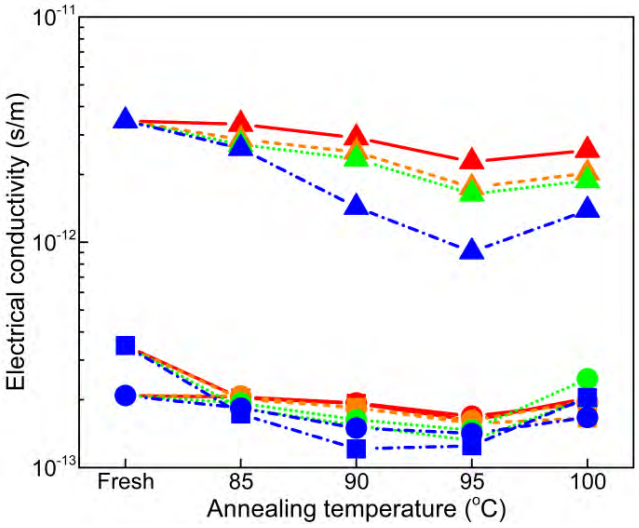

(a) Electrical conductivity from DC current

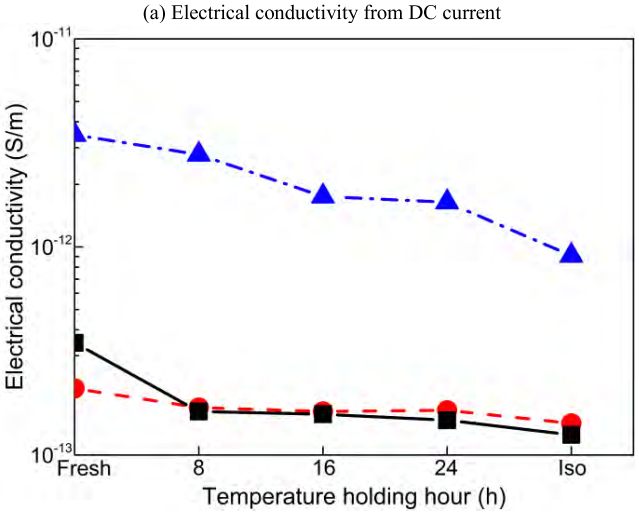

(b) Electrical conductivity for the samples annealed at 95 ℃

FIGURE 12. Electrical conductivity σ_{DC} as a function of annealing temperature. Solid symbols (■, ●, ▲) represent XLPE-0, XLPE-15, and XLPE-30. Solid line (——): S-1, short dash line (— —): S-2, short dot line (.....): S-3, short dash dot line (— . —): S-4. Iso is the abbreviation of isothermal treatment.

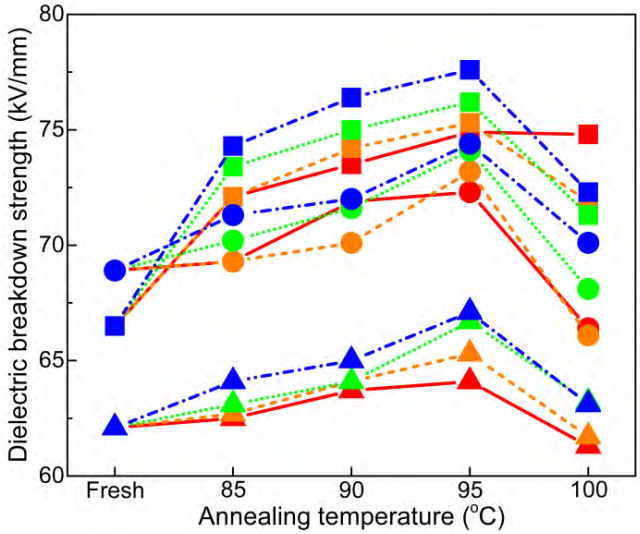

(a) Dielectric breakdown strength of all samples

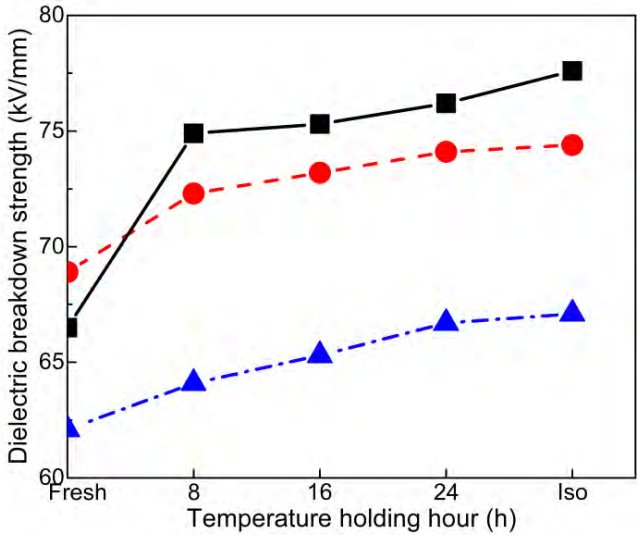

(b) Dielectric breakdown strength for the samples annealed at 95 ℃

FIGURE 13. Dielectric breakdown strength E_B as a function of annealing temperature. Solid symbols (■, ●, ▲) represent XLPE-0, XLPE-15, XLPE-30. Solid line (——): S-1, short dash line (— —): S-2, short dot line (.....): S-3, short dash dot line (— . —): S-4. Iso is the abbreviation of isothermal treatment.

to thicker lamellae, thereby hindering charge transport in the crystal region and increasing the dielectric breakdown strength [34], [35].

D. EFFECTS OF ANNEALING ON THE PERFORMANCE OF RETIRED CABLES

The results of the FTIR spectra shown in Figure 3 and 4 depict the molecular chain damage in the two retired cables, which scales linearly with the cable service year. The measured values, including the crystallinity, melting point, lamellar thickness, melting range, electrical conductivity, and dielectric breakdown strength illustrate that the most serious degradation occurred in XLPE-30.

For the samples annealed at different temperatures, the effect of annealing on the cable performance can be divided into three phases. For annealing temperatures of 85 and 90 °C, the improvements in the thermal and electrical performance in the three samples are proportional to the annealing temperature. When the samples are annealed at 95 °C, the annealing show the best effect for the three samples, and the optimal values of all the measured parameters are observed. Moreover, the annealing temperature of 100 °C negatively affects the thermal and electrical properties.

In summary, the different heat treatments considered in this study equally contribute to the changes in the thermal and electrical properties of the three samples. The optimal values of the melting point, crystallinity, lamellar thickness, electrical conductivity, and dielectric breakdown strength occur when the samples are annealed at 95 °C. When the samples are annealed at this temperature, a narrower melting range, lower electrical conductivity, and larger crystallinity, lamellar thickness, melting point, and dielectric breakdown strength

are observed with the increasing T_h. Furthermore, these heat treatments lasted for hundreds of hours and did not further damage the molecular chain.

The above measurements and results provide a feasible method by which heat treatment could contribute to improvements in the thermal and electrical properties for XLPE sheets from retired cables, though XLPE-15 and XLPE-30 suffered from serious degradation. While the research and the obtained results based on XLPE sheets do not sufficiently support their use in a cable, the thermal and electrical properties in each position of the insulation layer could be improved. If it is to be used in a transmission cable line, further research on the heat treatment of coaxial cables is needed. Several cables with different service year should be selected, to built-up small simulation circles. Then, heat treatment similar to the cable operation is performed, and the effects on the improvements in the thermal and electrical properties in each position in the insulation layer would be checked by multiple tests. Finally, the heat treatment would be performed on several on-site transmission cables to testify the feasibility of heat treatment for improvements in the electrical properties of the cable.

IV. CONCLUSION

Several heat treatments were performed on three cables that operated for 0, 15, and 30 years without records of overheating. Although the two retired cables suffered insulation degradation, the annealing treatment on the XLPE insulation remained effective. The optimal values of the melting point, crystallinity, melting range, lamellar thickness, electrical conductivity, and dielectric breakdown strength were observed when the samples were annealed at 95 °C. Longer temperature holding hour was further enhanced the thermal and electrical properties when the samples were annealed at this optimum point.

Further research will be conducted on coaxial cables, to explore and verify the improvement in the thermal and electrical properties in each position of the cable insulation. Finally, a feasible method will be proposed for the rejuvenation of on-site transmission cable by heat treatment.

REFERENCES

[1] F. Aras, V. Alekperov, N. Can, and H. Kirkici, "Aging of 154 kV underground power cable insulation under combined thermal and electrical stresses," *IEEE Elect. Insul. Mag.*, vol. 23, no. 5, pp. 25–33, Sep./Oct. 2007.

[2] R. Liu and S. Boggs, "Cable life and the cost of risk," *IEEE Elect. Insul. Mag.*, vol. 25, no. 2, pp. 13–19, Mar. 2009.

[3] J. C. Fothergill, G. C. Montanari, G. C. Stevens, C. Laurent, G. Teyssedre, L. A. Dissado, U. H. Nilsson, and G. Platbrood, "Electrical, microstructural, physical and chemical characterization of HV XLPE cable peelings for an electrical aging diagnostic data base," *IEEE Trans. Dielectr. Electr. Insul.*, vol. 10, no. 3, pp. 514–527, Jun. 2003.

[4] G. Mazzanti, "The combination of electro-thermal stress, load cycling and thermal transients and its effects on the life of high voltage ac cables," *IEEE Trans. Dielectr. Electr. Insul.*, vol. 16, no. 4, pp. 1168–1179, Aug. 2009.

[5] A. Tzimas, S. Rowland, L. A. Dissado, M. Fu, and U. H. Nilsson, "Effect of long-time electrical and thermal stresses upon the endurance capability of cable insulation material," *IEEE Trans. Dielectr. Electr. Insul.*, vol. 16, no. 5, pp. 1436–1443, Oct. 2009.

[6] N. Hozumi, M. Ishida, T. Okamoto, and H. Fukagawa, "The influence of morphology on electrical tree initiation in the polyethylene under AC and impulse voltages," in *Proc. IEEE 2nd Int. Conf. Properties Appl. Dielectr. Mater.*, Beijing, China, Sep. 1988, pp. 481–485.

[7] Y. Song and Q. Zheng, "Influence of annealing on conduction of high-density polyethylene/carbon black composite," *J. Appl. Polym. Sci.*, vol. 105, no. 2, pp. 710–717, 2007.

[8] H. Ghorbani, M. Saltzer, F. Abid, and H. Edin, "Effect of heat-treatment and sample preparation on physical properties of XLPE DC cable insulation material," *IEEE Trans. Dielectr. Electr. Insul.*, vol. 23, no. 5, pp. 2508–2516, Oct. 2016.

[9] Y. Xu, P. Luo, M. Xu, and T. Sun, "Investigation on insulation material morphological structure of 110 and 220 kV XLPE retired cables for reusing," *IEEE Trans. Dielectr. Electr. Insul.*, vol. 21, no. 4, pp. 1687–1696, Aug. 2014.

[10] W. Li, J. Li, X. Wang, S. Li, G. Chen, J. Zhao, and B. Ouyang, "Physicochemical origin of space charge dynamics for aged XLPE cable insulation," *IEEE Trans. Dielectr. Electr. Insul.*, vol. 21, no. 2, pp. 809–820, Apr. 2014.

[11] Y. L. Chong, G. Chen, I. L. Hosier, A. S. Vaughan, and Y. F. F. Ho, "Heat treatment of cross-linked polyethylene and its effect on morphology and space charge evolution," *IEEE Trans. Dielectr. Electr. Insul.*, vol. 12, no. 6, pp. 1209–1221, Dec. 2005.

[12] C. Katz and W. Zenger, "Service aged 69 and 115 kV XLPE cables," *IEEE Trans. Power Del.*, vol. 14, no. 3, pp. 685–689, Jul. 1999.

[13] G. Mazzanti, "Analysis of the combined effects of load cycling, thermal transients, and electrothermal stress on life expectancy of high-voltage AC cables," *IEEE Trans. Power Del.*, vol. 22, no. 4, pp. 2000–2009, Oct. 2007.

[14] J. H. Neher, "The temperature rise of buried cables and pipes," *Trans. Amer. Inst. Elect. Eng.*, vol. 68, no. 1, pp. 9–21, Jul. 1949.

[15] J. V. Gulmine and L. Akcelrud, "FTIR characterization of aged XLPE," *Polymer Test.*, vol. 25, no. 7, pp. 932–942, 2006.

[16] M. Mohammadhosseini and R. Jahanmardi, "Investigating effect of ferric stearate on stabilization efficiency of a phenolic antioxidant during thermal oxidation of polyethylene," *Iranian Polym. J.*, vol. 23, no. 10, pp. 801–807, 2014.

[17] P. Hyvönen, "Prediction of insulation degradation of distribution power cables based on chemical analysis and electrical measurements," Ph.D. dissertation, Dept. Elect. Eng., Helsinki Univ. Technol., Espoo, Finland, Jun. 2008.

[18] A. C. Albertsson, S. O. Andersson, and S. Karlsson, "The mechanism of biodegradation of polyethylene," *Polym. Degradation Stability*, vol. 18, no. 1, pp. 73–87, 1987.

[19] W. Mao and J. Jia, "Recrystallization in the oriented isotactic polypropylene during annealing," *J. Wuhan Univ. Sci. Technol.*, vol. 31, no. 2, pp. 394–398, 2008.

[20] N. Basu, A. Osichow, S. Mecking, and G. Reiter, "Morphological changes during annealing of polyethylene nanocrystals," *Eur. Phys. J. E*, vol. 35, no. 3, p. 18, 2012.

[21] B. Wunderlich, *Thermal Analysis of Polymeric Materials*. Berlin, Germany: Springer, 2005, ch. 2.

[22] B. Wunderlich and C. M. Cormier, "Heat of fusion of polyethylene," *J. Polym. Sci. A, Polym. Phys.*, vol. 5, no. 5, pp. 987–988, 1967.

[23] L. Contat-Rodrigo and A. R. Greus, "Biodegradation studies of LDPE filled with biodegradable additives: Morphological changes. I," *J. Appl. Polym. Sci.*, vol. 83, pp. 1683–1691, Feb. 2002.

[24] X. Jin, X. Xu, X. Zhang, and Y. Yin, "Determination of the PCM melting temperature range using DSC," *Thermochim. Acta*, vol. 595, pp. 17–21, Nov. 2014.

[25] D. W. van Krevelen and K. te Nijenhuis, *Properties of Polymers*. Amsterdam, The Netherlands: Elsevier, 2009, ch. 19.

[26] T. Yamamoto, "Molecular dynamics simulations of steady-state crystal growth and homogeneous nucleation in polyethylene-like polymer," *J. Chem. Phys.*, vol. 129, no. 18, 2008, Art. no. 184903.

[27] W. Wang, G. Zhao, X. Wu, and Z. Zhai, "The effect of high temperature annealing process on crystallization process of polypropylene, mechanical properties, and surface quality of plastic parts," *J. Appl. Polym. Sci.*, vol. 132, no. 46, p. 42773, 2015.

[28] K. C. Kao, *Dielectric Phenomena in Solids*. San Diego, CA, USA: Elsevier, 2004, pp. 323–341.

[29] R. J. Klein, S. Zhang, S. Dou, B. H. Jones, R. H. Colby, and J. Runt, "Modeling electrode polarization in dielectric spectroscopy: Ion mobility and mobile ion concentration of single-ion polymer electrolytes," *J. Chem. Phys.*, vol. 124, no. 14, 2006, Art. no. 144903.

[30] D. Min, C. Yan, Y. Huang, S. Li, and Y. Ohki, "Dielectric and carrier transport properties of silicone rubber degraded by gamma irradiation," *Polymers*, vol. 9, no. 10, pp. 533–548, 2017.
[31] R. Bodega, G. C. Montanari, and P. H. F. Morshuis, "Conduction current measurements on XLPE and EPR insulation," in *Proc. IEEE Conf. Elect. Insul. Dielectr. Phenomena*, Oct. 2004, pp. 101–105.
[32] Y. Masuzaki, Y. Suzuki, and Y. Ohki, "Superior high-temperature dielectric properties of dicyclopentadiene resin," *IEEE Trans. Dielectr. Electr. Insul.*, vol. 23, no. 5, pp. 3078–3085, Oct. 2016.
[33] G. Chen, M. Fu, X. Z. Liu, and L. S. Zhong, "AC aging and space-charge characteristics in low-density polyethylene polymeric insulation," *J. Appl. Phys.*, vol. 97, no. 8, pp. 083713-1–083713-7, 2005.
[34] M. Araoka, H. Yoneda, and Y. Ohki, "Dielectric breakdown of new type polymerized polyethylene using a single-site catalyst," *IEEE Trans. Dielectr. Electr. Insul.*, vol. 6, no. 3, pp. 326–330, Jun. 1999.
[35] Y. F. F. Ho, G. Chen, A. E. Davies, S. G. Swingler, S. J. Sutton, R. N. Hampton, and S. Hobdell, "Measurement of space charge in XLPE insulation under 50 Hz ac electric stresses using the LIPP method," *IEEE Trans. Dielectr. Electr. Insul.*, vol. 9, no. 3, pp. 362–370, Jun. 2002.

YUE XIE received the B.Eng. degree in electrical engineering from Wuhan Polytechnic University, Wuhan, China, in 2013. He is currently pursuing the Ph.D. degree in electrical engineering with the South China University of Technology, Guangzhou, China. His research interests include degradation mechanism of polymer dielectric materials and aging assessment of XLPE cable.

YIFENG ZHAO received the B.Eng. degree in electrical engineering from Wuhan Qingchuan University, Wuhan, China, in 2017. He is currently pursuing the M.Eng. degree in electrical engineering from the South China University of Technology, Guangzhou, China. His research interests include degradation mechanism of polymer dielectric materials and aging assessment of XLPE cable.

GANG LIU received the B.Eng., M.Eng., and Ph.D. degrees in electrical engineering from Xi'an Jiaotong University, Xi'an, China, in 1991, 1994, and 1998, respectively. He is currently an Associate Professor with the School of Electric Power, South China University of Technology, Guangzhou, China. His research interests include ampacity assessment and fault diagnosis of electrical equipments, and lightning protection of transmission line.

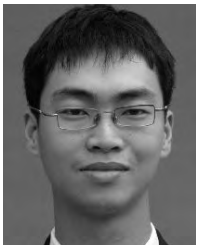

JIASHENG HUANG received the B.Eng. degree in electrical engineering from the Guangdong University of Technology, Guangzhou, China, in 2004. Since 2004, he has been an Engineer with Guangzhou Power Supply Company Ltd., Guangzhou. His research interest includes failure diagnose of transmission cables.

LICHENG LI received the B.Eng. degree in electrical engineering from Tsinghua University, China, in 1967. He is currently an Academician of the Chinese Academy of Engineering, and a Professor and a Doctoral Supervisor with the South China University of Technology. He is also the Secretary of the Expert Committee and China Southern Power Grid.